Charge-transfer Character in the Intramolecular Hydrogen Bond: Electronic Structures and Spectra of Hydrogen Maleate Anion and Related Molecules

Hiroshi MORITA, Kiyokazu FUKE, and Saburo NAGAKURA

The Institute for Solid State Physics, The University of Tokyo, Roppongi, Minato, Tokyo 106

(Received October 18, 1976)

Ultraviolet absorption spectra were measured with aqueous solutions of maleic acid (H_2M) at various pH values and in concentrated sulfuric acid solutions. With the aid of the theoretical calculations of electronic structures by the modified CNDO-CI method, relatively strong bands observed at 193.5 nm for H_2M, at 210.0 nm for the hydrogen maleate anion (HM^-), and at 202.8 and ≈230 nm for the dinegative ion (M^{2-}) are assigned to the π–π^* transition bands. Special attention was paid to the charge-transfer (CT) character (pertinent to the strong intramolecular hydrogen bond) in the excited states of HM^-. Configuration analysis of the wave functions revealed us that the first π–π^* band of HM^- covered by the much stronger 210 nm band is rich in the CT character pertinent to the hydrogen bond.

In some hydrogen-bonded systems (X–H···Y), the charge-transfer (CT) force between a proton donor (X–H) and a proton acceptor (Y) has been recognized to be important as well as the electrostatic and exchange repulsion forces.[1-6] On the basis of the CT mechanism, the CT band characteristic of hydrogen bond is expected to appear in the ultraviolet (UV) or vacuum ultraviolet (VUV) region, and observation of the band is a direct proof of the CT mechanism of hydrogen bond.

The hydrogen maleate anion (HM^-) has a symmetrical intramolecular hydrogen bond ($(O–H–O)^-$) as revealed from the X-ray diffraction analysis[7] and from the studies by infrared spectroscopy.[8-10] One of the present authors observed an electronic absorption band of HM^- in aqueous solution at ≈210 nm and determined the direction of the transition moment (being parallel to the O–H–O bond) of the band.[11] From a theoretical calculation based on the π-electron approximation, the 210 nm band was suggested to be the CT band characteristic of the intramolecular hydrogen bond ($(O–H–O)^-$) of HM^-. Further theoretical studies have been carried out with the ground and excited states of HM^- by the non-empirical[12] and semi-empirical[13] methods. The potential energy curve of hydrogen bond calculated by the modified CNDO method[13] for HM^- agreed with the experimentally expected one.[8-10]

In the present study, in order to extend the previous works and to elucidate the electronic structures of the excited states of the hydrogen maleate anion, the absorption spectra of the maleic acid cation (H_3M^+), maleic acid (H_2M), HM^-, and maleate dinegative ion (M^{2-}) have been measured and their electronic structures have been calculated and analysed by the modified CNDO-CI method[14] combined with the configuration analysis method.[15] From the comparison between the theoretical and experimental results, the CT character (pertinent to the hydrogen bond) in some lower excited states of HM^- has been discussed in detail.

Experimental

Maleic acid (Wako G. R. grade) was purified by repeated recrystallizations from water. HM^- was prepared[10] by treating aqueous solution of maleic acid with potassium hydrogen carbonate ($KHCO_3$), and recrystallized three times from water. Methanol and acetonitrile (Wako spectrograde) were used as solvents without further purification. A buffer solution with pH=4.4 was prepared from aqueous solutions of acetic acid and sodium acetate.[16]

UV absorption spectra were measured with a Cary recording spectrophotometer model 14, a cell of 0.933 mm light path length being used. VUV absorption spectra were measured with a spectrophotometer constructed in our laboratory[17].

Theoretical

The electronic structures of H_3M^+, H_2M, HM^-, and M^{2-} were calculated by the modified CNDO-CI method presented in a previous paper.[14] The method has the characteristics that the semi-empirical electron repulsion, core resonance, and core potential integrals are separately evaluated for the σ- and π-orbitals. As in the case of formic and acrylic acids reported,[14] the one-center Coulomb repulsion integrals, γ's and bonding parameters, β^0's were commonly used for all the 2s and 2p atomic orbitals (AO) of the two oxygen atoms in the carboxyl group. Furthermore, in order to consider the effect of excess formal charge of the ions, the β^0 and γ values and the effective nuclear charge (Z) of the basis

TABLE 1. EFFECTIVE NUCLEAR CHARGE (Z), ONE-CENTER COULOMB REPULSION INTEGRAL (γ_{AA}(eV)), AND BONDING PARAMETER (β_A^0(eV)) FOR H, C, AND O ATOMS

	H	C		O[a]			
		σ-AO	π-AO	H_3M^+	H_2M	HM^-	M^{2-}
Z	1.2(1.0)[b]	3.25	3.25	4.64	4.55	4.46	4.38
γ_{AA}	12.85	13.22	10.60	18.23	17.89	17.55	17.20
β_A^0	−12.0(−9.0)[b]	−17.9	−12.9	−31.8	−27.0	−23.0	−17.9

a) Value being employed for both the σ- and π-AO's. b) Employed only for HM^-.

AO's of oxygen and the hydrogen-bonded hydrogen atoms were modified from those of the neutral H_2M molecule. The parameters finally used are tabulated in Table 1. In the configuration interaction (CI) calculation, 24 singly excited π–π^* and σ–σ^* configurations and 25 singly excited π–σ^* and σ–π^* configurations were taken into account.

Geometrical structures were taken for H_2M and HM^- from the X-ray crystal analysis data[7,18] and assumed for H_3M^+ and M^{2-} to be the same as those of H_2M and HM^-, respectively, except for the fact that the additional proton was attached or removed.

The configuration analysis[15] was applied to the ground and two excited (B_1 symmetry) states of HM^-. The molecular orbitals (MO) of M^{2-} and 1s orbital of the hydrogen-bonded hydrogen atom were adopted as the reference MO's. The ground state of HM^- was analysed by the ground and 92 singly excited π–π^* and σ–σ^* reference configurations (with A_1 symmetry) and by all the doubly excited reference configurations derived from the above configurations, and the excited states of HM^- were analysed by 93 singly excited π–π^* and σ–σ^* reference configurations (with B_1 symmetry) and 93×92 doubly excited reference configurations.

Results and Discussion

Figure 1 shows the absorption spectra of HM^- in aqueous buffer solution with pH=4.4 and of M^{2-} in aqueous KOH solution with pH=11.0, the spectrum of M^{2-} being tentatively resolved into two components.

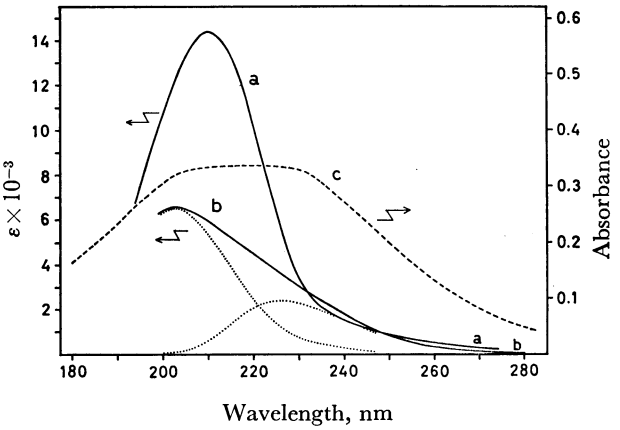

Fig. 1. Near and vacuum UV absorption spectra of (a) HM^- in aqueous buffer solution with pH=4.4, (b) M^{2-} in aqueous KOH solution with pH=11.0, and (c) HM^- crystalline powder. The composite band of M^{2-} is tentatively resolved by dotted lines.

This figure also shows the VUV spectrum observed with HM^- crystalline powder. Table 2 shows the transition energies, oscillator strengths, and directions of transition moments calculated by the modified CNDO-CI method, together with the observed values. Within the molecular (x-y) plane, the x-axis is parallel to the O–H–O hydrogen bond. From the comparison between the observed and calculated results, the 210.0 nm (5.90 eV) band of HM^- in aqueous solution and ≈220 nm band of HM^- crystalline powder can safely be assigned to the second

Table 2. Transition energies ($^1\Delta E$ (eV)), oscillator strengths (f), and directions of transition moments observed and calculated for HM^- and M^{2-}

HM^-						M^{2-}				
Assignment	Obsd $^1\Delta E$	Obsd f	Calcd $^1\Delta E$	Calcd f	Main config.[a]	Assignment	Obsd $^1\Delta E$	Obsd f	Calcd $^1\Delta E$	Calcd f
n–π^*			3.36	0.002 (z) [b]	22—23	n–π^*			3.00	0.001 (z) [b]
n–π^*			3.98	0	19—23	n–π^*			3.51	0.000 (z)
n–π^*			4.17	0.000 (z)	21—23	n–π^*			3.57	0
n–π^*			5.77	0	22—24 16—23	n–π^*			3.73	0
						π–π^*			5.31	0.021 (x)
n–π^*			6.05	0.002 (z)	22—25 19—24	π–π^*	≈5.4	≈0.06	5.38	0.101 (y)
π–π^*			6.32	0.063 (x)	17—23 22—26	n–π^*			5.73	0.009 (z)
						n–π^*			6.06	0
n–π^*			6.71	0	22—24 19—23 19—25	σ–π^*			6.79	0
						π–π^*	6.11	0.18	6.83	0.543 (x)
π–π^*	5.90	0.42	6.73	0.626 (x)	20—23	n–π^*			6.91	0.000 (z)
π–π^*			6.81	0.058 (y)	18—23	π–σ^*			7.09	0.000 (z)
n–π^*			7.82	0.001 (z)	22—25 21—25	π–σ^*			7.09	0
						n–π^*			7.14	0
π–π^*			8.13	0.729 (x)	17—23 22—26	π–π^*			7.40	0.439 (x)
						π–π^*			7.53	0.166 (y)
σ–π^*			8.29	0	16—23 15—23					

a) Main electron configurations of the respective excited states are shown. b) The direction of the transition moment is shown in the parentheses, the x-axis being taken to be parallel to the O–H–O bond within the molecular (x-y) plane.

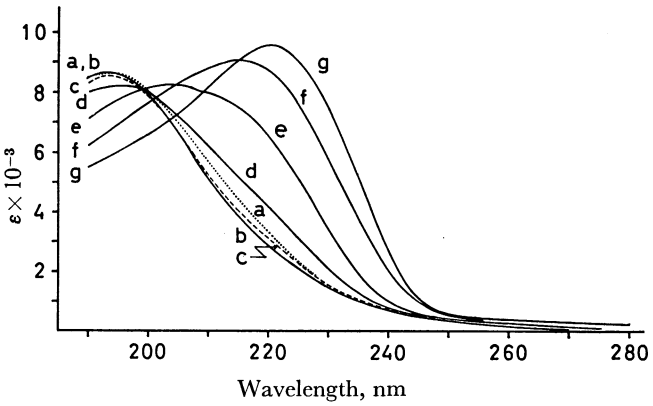

Fig. 2. UV absorption spectra of maleic acid in (a) 1.78% (dotted line), (b) 8.64%, (c) 24.3% (broken line), (d) 42.5%, (e) 62.5%, (f) 78.2%, and (g) 90.9% sulfuric acid.

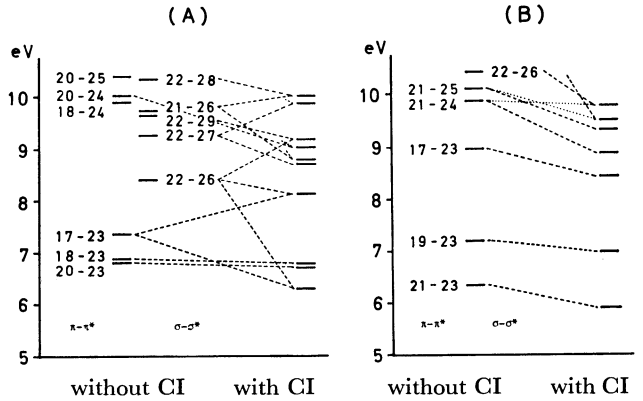

Fig. 3. Energy levels calculated with and without CI treatment for some lower π–π^* and σ–σ^* excited states of (A) HM^- and (B) H_2M.

π–π^* transition (calculated at 6.73 eV), whereas the ≈230 nm (≈5.4 eV) and 202.8 nm (6.11 eV) bands of M^{2-}, to the second and third π–π^* transitions (calculated at 5.38 and 6.83 eV), respectively. The theoretical results indicate that the first π–π^* band is covered by the stronger second (and third) π–π^* band(s) for both HM^- and M^{2-}.

Figure 2 shows the UV absorption spectra measured with the sulfuric acid (H_2SO_4) solutions of maleic acid. From the dependency of the spectrum on the sulfuric acid concentration, spectrum b in 8.6% H_2SO_4 solution can be ascribed to the spectrum of H_2M. The theoretical result in Table 3 shows that the 193.5 nm (6.41 eV) band of H_2M is assigned to the first π–π^* transition (calculated at 5.87 eV). In more concentrated sulfuric acid, the spectrum shifts to longer wavelengths, showing a strong band at 220.5 nm (5.62 eV) (curve g in Fig. 2). The spectra of the concentrated sulfuric acid solutions e, f, and g show practically no change even after 15 days. Moreover, dilution of the 90.9% H_2SO_4 solution of maleic acid (solution g) with water gives a spectrum similar to that of the sulfuric acid solution of the corresponding acidity. These facts indicate that the species having the absorption band at 220.5 nm in concentrated sulfuric acid solution is not a reaction product but a cation in equilibrium with sulfuric acid; H_3M^+ or the acylium ion as observed with the concentrated H_2SO_4 solution of mesitoic acid.[19]

Table 3. Transition energies ($^1\Delta E$(eV)) and oscillator strengths (f) observed and calculated for H_2M and H_3M^+

H_2M					H_3M^+		
Assignment	Obsd $^1\Delta E$	Obsd f	Calcd $^1\Delta E$	Calcd f	Assignment	Calcd $^1\Delta E$	Calcd f
n–π^*			3.28	0.003	n–π^*	3.90	0.003
n–π^*			3.92	0.000_6	π–π^*	6.20	0.335
n–π^*			5.84	0.000_4	n–π^*	6.44	0.001
π–π^*	6.41	0.35	5.87	0.489	σ–π^*	6.84	0.000_1
σ–π^*			6.66	0.000_4	σ–π^*	7.55	0.000_3
π–π^*			6.96	0.013	π–π^*	8.02	0.293
n–π^*			7.01	0.000_7	n–π^*	8.40	0.000
σ–π^*			7.60	0.003	σ–π^*	8.57	0.000_6
π–π^*			8.40	0.415	π–π^*	9.09	0.084
π–π^*			8.84	0.123	π–σ^*	9.25	0.004
π–σ^*			8.85	0.002	π–π^*	9.36	0.576
n–π^*			8.90	0.000_7	σ–π^*	9.99	0.000_8
π–σ^*			9.25	0.028	n–σ^*	10.24	0.040
π–π^*			9.30	0.169			
n–σ^*			9.48	0.069			

Let us investigate the electronic structure of HM^- in more detail. Figure 3 shows the energy levels calculated for some lower π–π^* and σ–σ^* excited states of HM^- compared with those of H_2M. In the figure, a singly excited configuration i–j represents one electron excitation from the i-th occupied MO to the j-th vacant MO. The shapes of MO's of HM^- are schematically shown in Fig. 4. The CT character pertinent to the intramolecular

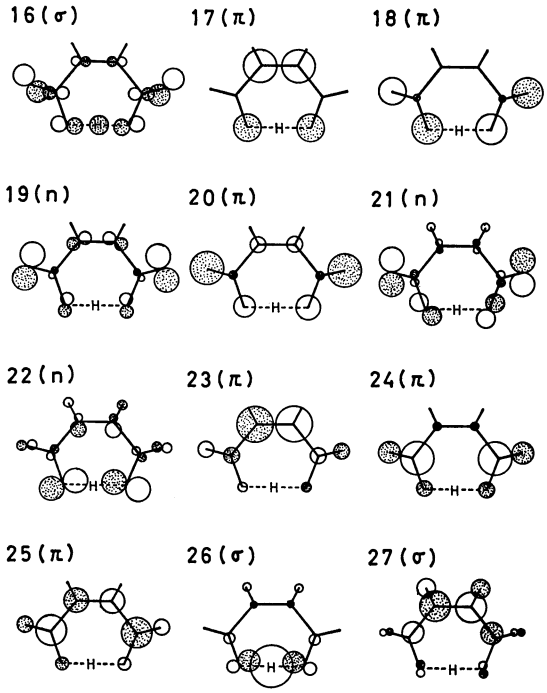

Fig. 4. Schematic shapes of some occupied and vacant MO's of HM^-. The 22th MO is the highest occupied one.

Table 4. Results of the configuration analysis (weights) for the ground and the first and second π–π^* excited states of HM^-

Structure	Reference configuration[a,b]	State		
		Ground	1 st π–π^*	2 nd π–π^*
$(OH^-O^+)^- + (O^+H^-O)^-$[c]	i,j-35, 35	0.1095	—	—
$(OH^-O^+)^- - (O^+H^-O)^-$	i,j-35, 35	—	0.1058 (0.1617)[d]	0.0058 (0.0067)[d]
$(O\text{–}H\cdots O)^- + (O\cdots H\text{–}O)^-$	i-35	0.4093	—	—
	i-35+π–π^*[e]	0.0272	0.2577 (0.1672)	0.4045 (0.3981)
	i-35+σ–σ^*[e]	0.0154	0.0124 (0.0227)	0.0057 (0.0108)
	(Total for sym. covalent structure)	(0.4519)	(0.2701 (0.1899))	(0.4102 (0.4089))
$(O\text{–}H\cdots O)^- - (O\cdots H\text{–}O)^-$	i-35	—	0.1978 (0.3023)	0.0109 (0.0125)
	i-35+π–π^*[e]	—	0.0131 (0.0200)	0.0007 (0.0008)
	i-35+σ–σ^*[e]	—	0.0079 (0.0122)	0.0004 (0.0004)
	(Total for antisym. covalent structure)		(0.2188 (0.3345))	(0.0120 (0.0137))
$O\text{–}H^+O^-$	G^0[f]	0.3825	—	—
	π–π^*[g]	0.0254	0.2408 (0.1562)	0.3780 (0.3721)
	σ–σ^*[g]	0.0172	0.0154 (0.0274)	0.0058 (0.0107)
	i,j-k,l	0.0024	0.0237 (0.0173)	0.0341 (0.0341)
	(Total for $O\text{–}H^+O^-$ structure)	(0.4275)	(0.2799 (0.2009))	(0.4179 (0.4169))
	Total	0.9889	0.8746 (0.8870)	0.8459 (0.8462)

a) i and j denote the 22 occupied MO's of M^{2-}, and k and l, the 12 vacant MO's of M^{2-}. The 1s orbital of hydrogen-bonded hydrogen is numbered as the 35th vacant orbital. b) i–k and i,j-k,l denote the singly and doubly excited reference configurations, respectively. c) The ionic structure, $[(O^+H^-O)^- + (OH^-O^+)]$ is also involved. d) The result for the case where the excitation energies of all the CT and σ–σ^* configurations are lowered by 1.0 eV in the CI treatment is listed in the column (with parentheses). e) Doubly excited configurations, i,j-k, 35. f) The ground reference configuration coincides with the ground state of M^{2-}. g) Singly excited configurations, i-k.

hydrogen bond corresponds to the transition from the nonbonding orbital to the antibonding orbital in the hydrogen bond. The 21—26 and 22—26 configurations are easily seen to have the CT character pertinent to the hydrogen bond. The energy levels of the CT configurations calculated for HM^- are $\approx$3 eV lower than those for the corresponding CT configurations of H_2M. As is illustrated in Fig. 3, the CT configuration 22—26 of HM^- interacts strongly with the 17—23 π–π^* configuration. Consequently, the first and fourth π–π^* excited states of HM^- turn out to be considerably rich in the CT character pertinent to the hydrogen bond.

The conclusion was further clarified by the configuration analysis for the first π–π^* excited state of HM^-; the result is tabulated in Table 4, together with the results for the ground and the second π–π^* excited (assigned to the 210.0 nm band) states. Because of the symmetrical hydrogen bond in HM^-, the CT structure corresponds to the antisymmetric covalent structure, $[(O\text{–}H\cdots O)^- - (O\cdots H\text{–}O)^-]$ and the antisymmetric ionic structure, $[(OH^-O^+)^- - (O^+H^-O)^-]$. As is shown in Table 4, the antisymmetric covalent and ionic structures contribute considerably ($\approx$32%) to the first π–π^* excited state, revealing that the first π–π^* excited state is rich in the CT character in the hydrogen bond. Table 4 shows also the result for the case where the excitation energies of all the CT and σ–σ^* configurations are lowered by 1.0 eV in the CI treatment. The result shows that the quantitative CT character is sensitive to

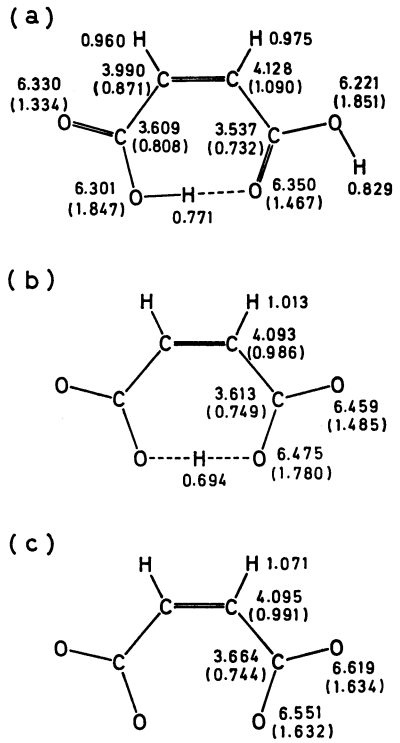

Fig. 5. Total and π-(in parentheses) electron densities calculated for the ground states of (a) H_2M, (b) HM^-, and (c) M^{2-}.

the relative position of the π–π^* (17—23) and CT (22—26) configurations; the CT character of the first π–π^* excited state increases to $\approx$50% by the energy lowering of the CT configuration.

The electron densities for the ground states of H_2M, HM^-, and M^{2-} are shown in Fig. 5. The excess formal charge in HM^- and M^{2-} is mainly distributed on the oxygen atoms.

References

1) C. A. Coulson, *Research (London)*, **10**, 149 (1957).
2) S. Bratož, "Advances in Quantum Chemistry," Vol. 3, ed by P.O. Löwdin, Academic Press, New York (1967), p. 209.
3) H. Tsubomura, *Bull. Chem. Soc. Jpn.*, **27**, 445 (1954); *J. Chem. Phys.*, **23**, 2130 (1955); *ibid.*, **24**, 927 (1956).
4) K. Nukasawa, J. Tanaka, and S. Nagakura, *J. Phys. Soc. Jpn.*, **8**, 792 (1953); S. Nagakura and M. Gouterman, *J. Chem. Phys.*, **26**, 881 (1957).
5) M. Weissmann and N. V. Cohan, *J. Chem. Phys.*, **43**, 119 (1965).
6) F. B. van Duijneveldt and J. N. Murrell, *J. Chem. Phys.*, **46**, 1759 (1967).
7) S. F. Darlow and W. Cochran, *Acta Crystallogr.*, **14**, 1250 (1961); S.F. Darlow, *ibid.*, **14**, 1257 (1961).
8) H. M. E. Cardwell, J. D. Dunitz, and L. E. Orgel, *J. Chem. Soc.*, **1953**, 3740.
9) R. Blinc, D. Hadži, and A. Novak, *Z. Electrochem.*, **64**, 566 (1960).
10) K. Nakamoto, Y. A. Sarma, and G. T. Behnke, *J. Chem. Phys.*, **42**, 1662 (1965).
11) S. Nagakura, *J. Chim. Phys.*, **61**, 217 (1964).
12) K. Morokuma, S. Iwata, and W. A. Lathan, "The World of Quantum Chemistry," ed by R. Daudel and B. Pullman, D. Reidel, Dordrecht, Holland (1974), p. 277.
13) H. Morita and S. Nagakura, *Theor. Chim. Acta*, **27**, 325 (1972).
14) H. Morita, K. Fuke, and S. Nagakura, *Bull. Chem. Soc. Jpn.*, **49**, 922 (1976).
15) H. Baba, S. Suzuki, and T. Takemura, *J. Chem. Phys.*, **50**, 2078 (1969).
16) "International Critical Tables," Vol. 1, National Research Council, McGraw-Hill, New York (1926), p. 84.
17) K. Kaya and S. Nagakura, *J. Mol. Spectrosc.*, **44**, 279 (1972).
18) M. Shahat, *Acta Crystallogr.*, **5**, 763 (1952).
19) H. Hosoya and S. Nagakura, *Spectrochim. Acta*, **17**, 324 (1961).